

See discussions, stats, and author profiles for this publication at: <https://www.researchgate.net/publication/236884503>

Dynamic Hydrogels with an Environmental Adaptive Self-Healing Ability and Dual Responsive Sol–Gel Transitions

ARTICLE in ACS MACRO LETTERS · JANUARY 2012

Impact Factor: 5.76 · DOI: 10.1021/mz200195n

CITATIONS

74

READS

242

8 AUTHORS, INCLUDING:



Guohua Deng

South China University of Technology

14 PUBLICATIONS 571 CITATIONS

[SEE PROFILE](#)



Weixiang Sun

South China University of Technology

22 PUBLICATIONS 184 CITATIONS

[SEE PROFILE](#)

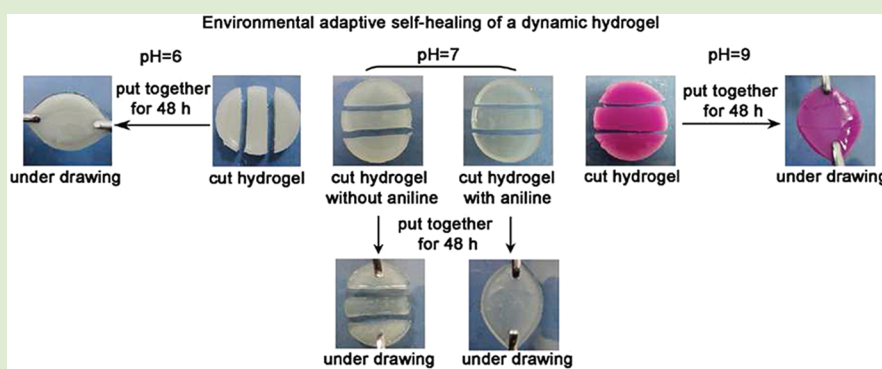
Dynamic Hydrogels with an Environmental Adaptive Self-Healing Ability and Dual Responsive Sol–Gel Transitions

Guohua Deng,*[†] Fuya Li,[†] Hongxia Yu,[†] Fuyong Liu,[‡] Chenyang Liu,*[‡] Weixiang Sun,[†] Huanfeng Jiang,[†] and Yongming Chen*[‡]

[†]School of Chemistry and Chemical Engineering, South China University of Technology, Guangzhou 510640, P. R. China

[‡]State Key Laboratory of Polymer Physics and Chemistry, Institute of Chemistry, The Chinese Academy of Sciences, Beijing 100190, P. R. China

Supporting Information



ABSTRACT: Dynamic polymer hydrogels with an environmental adaptive self-healing ability and dual responsive sol–gel transitions were prepared by combining acylhydrazone and disulfide bonds together in the same system. The hydrogel can automatically repair damage to it under both acidic (pH 3 and 6) and basic (pH 9) conditions through acylhydrazone exchange or disulfide exchange reactions. However, the hydrogel is not self-healable at pH 7 because both bonds are kinetically locked, whereas the hydrogel gains self-healing ability by accelerating acylhydrazone exchange with the help of catalytic aniline. All of the self-healing processes are demonstrated to be effective without an external stimulus at room temperature in air. The hydrogel also displays unique reversible sol–gel transitions in response to both pH (HCl/triethylamine) and redox (DTT/H₂O₂) triggers.

Self-healing is a fascinating property of living creatures. A living body can automatically repair damage by activating the self-healing process and, thus, restore certain destroyed functions. This striking feature has inspired researchers to design self-healable synthetic polymers.^{1,2} Over the past decade, two main approaches, based on irreversible and reversible mechanisms, respectively, have been developed for this purpose.¹ A typical irreversible system based on the ring-opening metathesis polymerization (ROMP) mechanism was reported by White et al. in 2001.³ Some complex systems, such as microvascular network containing systems,⁴ have been developed, but the healing mechanism remains irreversible, which is a drawback for such systems.

In contrast, a reversible system can repeat the self-healing process for numerous cycles when noncovalent bonds or dynamic covalent bonds are used.¹ Such noncovalent and dynamic covalent bonding^{5–7} can be reversed under equilibrium controls. Modified by external stimuli or through continuous component exchange, noncovalent and dynamic covalent bonds can be reorganized or reshuffled to cure the system. A recent example is a self-healable rubber based on hydrogen bonding.⁸ Other noncovalent bonding systems, such

as π – π stacking⁹ and ionic interactions,¹⁰ have also been reported. However, noncovalent bonding systems are often unstable.¹¹ Conversely, dynamic covalent bonding systems containing reversible but strong covalent bonds are desirable for structural healable polymeric materials. For example, systems employing Diels–Alder chemistry¹² and reshuffling reactions of trithiocarbonate units^{13,14} have been reported.

In our previous work, we reported a polymer organogel with reversible self-healing properties based on the dynamic chemistry of acylhydrazone bonds.¹⁵ This self-healing of the organogel was automatic without any external stimulus at room temperature in air. Because acylhydrazone bonds can be activated under mild acidic conditions⁶ or by catalytic aniline in neutral conditions,^{16,17} these bonds are compatible with physiological environments in biological systems. Therefore, acylhydrazone is suitable for constructing *self-healable hydrogels* for biological/medical applications. Comparable with the acylhydrazone bond, the disulfide bond, which biologically

Received: November 29, 2011

Accepted: January 3, 2012

Published: January 12, 2012



Scheme 1. Strategy for Constructing a Dynamic Hydrogel with an Environmental Adaptive Self-Healing Ability and Dual Responsive Sol–Gel Transitions Based on Acylhydrazone and Disulfide Chemistry

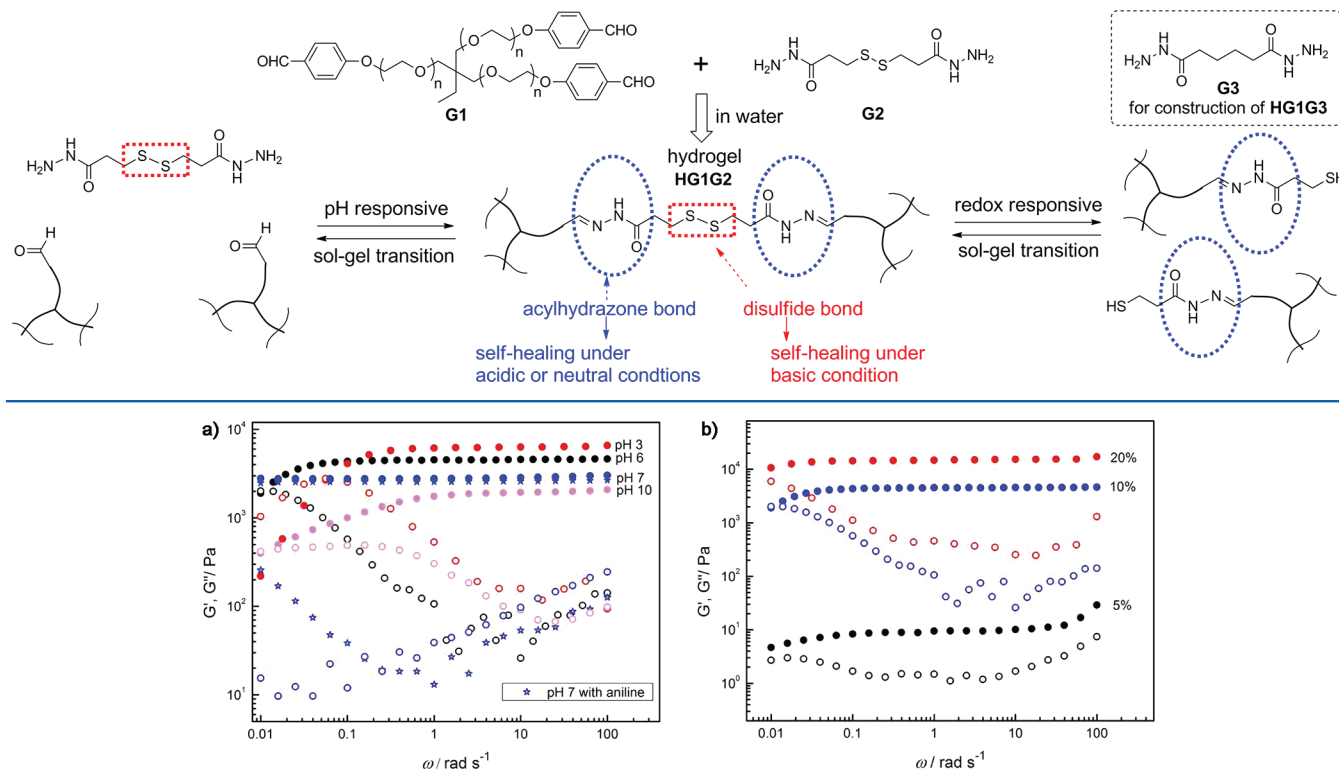


Figure 1. Rheological properties (25°C) of hydrogel HG1G2. (a) HG1G2 (10 wt %) at different pH values; (b) HG1G2 (pH 6) with different gelator concentrations. Solid symbols represent G' , and open symbols represent G'' .

occurs as another attractive dynamic covalent bond,⁶ is multiresponsive to pH, light, and redox conditions.¹⁸ In fact, systems based on disulfide bonds have been constructed, such as photoresponsive dynamers¹⁹ and self-healing rubber.²⁰ Moreover, acylhydrazone and disulfide exchange reactions were demonstrated to be compatible with each other and independently operational upon pH changes in a single system in water or other solvents.^{21–23} Thus, it would be interesting to incorporate the two dynamic bonds into the same polymer network to obtain a complex system with controllable multiresponsiveness.¹⁸

In this work, we synthesized a new self-healing hydrogel, containing both acylhydrazone and disulfide bonds, as shown in Scheme 1. This hydrogel can inherently select specific self-healing routes to adapt to different chemical environments. The hydrogel undergoes acylhydrazone exchange to repair damage in an acidic environment, while it undergoes disulfide exchange for self-healing in a basic environment. The hydrogel is not self-healable under neutral conditions because both dynamic bonds are kinetically locked.²² However, catalytic aniline added at preparation can accelerate the acylhydrazone exchange reaction,^{16,17} facilitating the hydrogel self-healing at pH 7. Our experiments illustrated that the self-healing processes are automatic without any external stimulus and repeatable at room temperature in air. Furthermore, the hydrogel is reversible in sol–gel transitions in response to both pH and redox conditions.

The hydrogel containing acylhydrazone and disulfide bonds, named HG1G2, was prepared from G1 and G2 (Scheme 1; for the synthetic method, see Supporting Information, SI). For comparison, the HG1G3 hydrogel, containing only the

acylhydrazone bonds, was prepared from G1 and G3 (Scheme 1). Gelation time for HG1G2 was dependent on pH and gelator concentration. By mixing G1 and G2 (with a total concentration of 10 wt %) in air-saturated pure water (pH 6) at room temperature, the gel formed after 5 min. At concentrations of 20 and 5 wt %, 2 and 10 min were required, respectively, to form the gels. In buffers with pH 7 and 4, it took 90 and 2.5 min, respectively, for HG1G2 (10 wt %) formation. The gelation time of HG1G3 was similar to that of HG1G2 under the same conditions.

After immersion in pure water (pH 6) for 72 h at room temperature, both HG1G2 and HG1G3 (pH 6) could not decompose as chemical gels. IR spectra of G1, G2, G3, HG1G2, and HG1G3 (SI, Figure S4) demonstrate that absorption from aldehyde groups at 1690 cm^{-1} in G1 becomes undetectable in both HG1G2 and HG1G3, while the absorptions from carbonyl groups in G2 (at 1636 cm^{-1}) and G3 (at 1632 cm^{-1}) display small shifts to 1639 cm^{-1} , indicating the formation of acylhydrazone bonds in the gels.

HG1G2 is opaque, but HG1G3 is transparent. After the hydrogels are freeze-dried, their SEM images (SI, Figure S5) exhibit different morphologies, demonstrating that the porous structures in the two hydrogels are different. Regularly scattered micropores were observed in HG1G3 (Figure S5b of the SI), but irregular and large domains were found in HG1G2 (Figure S5a of the SI). The reason for this difference may be related to the difference of gelator units from G2 and G3. In contrast to G3, G2 contains an additional $-S-S-$ group, which contributes hydrophobicity to the polymer chains and aggregates into microdomains in HG1G2, which scatters light.

Mechanical properties of HG1G2 under different conditions were studied by dynamic rheological measurements. In Figure 1a, the storage moduli, G' , and loss moduli, G'' , are presented as functions of frequency (ω) at a fixed strain, $\gamma = 1.0\%$, for HG1G2 (10 wt %) at different pH values (pH 3, 6, 7, and 10). For HG1G2 at pH 7, two pairs of G' and G'' curves are included in Figure 1a: one pair (blue circles) is from HG1G2 *without* aniline catalyst, and the other (blue stars) is from HG1G2 *with* aniline (5 μ L in 1 mL solution). At a high frequency regime, all samples display a solid-like characteristic, with $G' > G''$, as well as G' independent of frequency (showing a plateau). At a low frequency regime, HG1G2 at pH 3 and 6 displays frequency-dependent moduli: G' decreases and G'' increases with decreasing frequency. Therefore, the G'' curve intersects G' at approximately 0.06 rad/s for the sample at pH 3 (red symbols), and the well-known “terminal” regime ($G' \sim \omega^2$, $G'' \sim \omega$) is observed at lower frequencies. For the sample at pH 6 (black symbols), the crossover frequency (ω_{cross}) between G' and G'' is observed at approximately 0.01 rad/s. However, for HG1G2 at pH 7 *without* aniline (blue circles), G' displays a frequency-independent plateau, and G'' is much lower than G' during the entire frequency scope. Furthermore, unlike other G'' curves at pH 3 and 6, there is no trend showing that G'' would increase along with decreasing frequency at a low frequency regime.

It was previously reported that chemical gels formed by permanent covalent bonds display frequency-independent G' , while frequency-dependent G' and G'' are observed for gels containing reversible covalent bonds²⁴ and supramolecular networks formed by metal–ligand interactions.²⁵ At low frequencies, reversible gels exhibit fluid-like behavior (Figure 3a in ref 24) because the time scale probed is longer than the lifetime of the kinetically labile cross-links, thus allowing time for the network to restructure. At higher frequencies, where not enough time is provided for the labile cross-links to dissociate, elastic-like behavior dominates, displaying a frequency-independent G' plateau. Furthermore, the dissociation rate constant (k_d) of the reversible network can be estimated by the crossover frequency (ω_{cross}) of G' and G'' , as reported in the literature (i.e., $k_d \approx \omega_{\text{cross}}$, as shown in Figure 6a in ref 25). It is worth noting that k_d is not exactly equal to ω_{cross} because ω_{cross} has a weak dependence on concentration, which can be observed in Figure 3a in ref 24 or in Figure 1b in the present paper. Therefore, the dissociation rate constant k_d obtained from ω_{cross} increases with decreasing pH for HG1G2 dynamic hydrogels under acidic conditions, and the k_d of the sample at pH 7 *without* aniline is too small to be observed from rheological measurements. Under neutral conditions, both acylhydrazone and disulfide bonds are kinetically locked,²² so the hydrogel acts as a permanently cross-linked network. However, under acidic conditions, acylhydrazone bonds can dynamically break and reform, with the dissociation rate constant controlling the acylhydrazone exchange reaction and the self-healing speed. Therefore, the hydrogel displays good self-healing ability at pH 6 (or at pH 3). At pH 7, the hydrogel *without* aniline is not self-healable at ambient conditions, which is discussed below. The result that k_d increases with decreasing pH is also consistent with our previous observations that HCl can induce the gel–sol transition for the organogel based on the dynamic acylhydrazone bond.¹⁵

When catalytic aniline was added, the sample (blue stars) exhibits a different rheological behavior at pH 7 (Figure 1a). Although its G' displays a frequency-independent plateau, its G'' curve is very different from that of the sample *without* aniline:

after a minimum value, the G'' increases with decreasing frequency with a trend to intersect G' (Figure 1a). This crossover frequency (ω_{cross}) between G' and G'' is estimated to be approximately 0.0008 rad/s by superposing the data at pH 6 onto those at pH 7 *with* aniline due to the similar shapes of the G'' curves, which implies similar mechanisms of the dissociation reactions at different conditions (except pH 10) (SI, Figure S6).²⁵ These results confirm that aniline accelerates the acylhydrazone exchange reaction,^{16,17} and thus, the hydrogel at pH 7 *with* aniline gains self-healing ability (in contrast to the counterpart *without* aniline, in detail in the next section).

Under basic conditions (pH 10, purple symbols), the G' and G'' curves demonstrate slightly different features from those obtained under acidic conditions. G' deviates from the plateau region at approximately 1 rad/s, but the crossover frequency between G' and G'' appears at approximately 0.01 rad/s. Because the disulfide exchange reaction can be triggered by a base without catalysis by DTT (1,4-dithiothreitol) or other thiols,²⁶ the reversibility of the disulfide bond here is responsible for the frequency-dependent G' and G'' . Thus, the rheological properties of HG1G2 over the broad pH range presented in Figure 1a are conclusively in accordance with the dynamic chemistry of acylhydrazone and disulfide bonds in the same system.

Figure 1b shows the G' and G'' curves of HG1G2 hydrogels at pH 6 with different gelator concentrations (5, 10, and 20 wt %). The G' plateau increases with increasing gelator concentration, but the crossover frequency between G' and G'' (approximately 0.01 rad/s) is nearly independent of the gelator concentration. These features, arising from the reversible covalent bond gels, were reported by another group (Figure 3a in ref 24) and indicate that the k_d is a material constant at a given temperature and pH. In addition, the sample with 5 wt % gelator retains its gel state ($G' > G''$) but with very low strength. No gel formed when the gelator concentration was <5 wt %.

The adaptive self-healing properties, based on the dynamic chemistry of both acylhydrazone and disulfide bonds, were further studied, and our results are presented in Figure 2 (see also SI, Table S1). A plate of the HG1G2 hydrogel (10 wt %, pH 6) (Figure 2-1a) was cut into three pieces (Figure 2-1b), and then the pieces were placed closely together along the cut line in a container in air saturated with moisture. After incubation at room temperature for 48 h without any external stimulus (Figure 2-1c), the three pieces completely merged together and could not be forced to split along the dimly visible cut lines (Figure 2-1d). Under these acidic conditions, the acylhydrazone exchange reaction is responsible for the self-healing process.

At pH 7, HG1G2 could not self-heal in 48 h or even up to 7 days (Figure 2-2a–2d). This result is due to the fact that both acylhydrazone and disulfide bonds are kinetically locked under neutral conditions.²² However, when catalytic aniline (5 μ L for 1 mL solution) was added during hydrogel preparation, the HG1G2 gel plates (Figure 2-3b) self-healed into a whole piece in 48 h (Figure 2-3c,3d). This result is consistent with the dynamic rheological results in Figure 1a showing that aniline accelerates the acylhydrazone exchange reaction, and the hydrogel at pH 7 *with* aniline consequently gains self-healing ability.

Under more basic conditions, however, HG1G2 became healable. After immersion in a buffer solution (pH 9, with phenolphthalein as an indicator) for 24 h, a plate of HG1G2

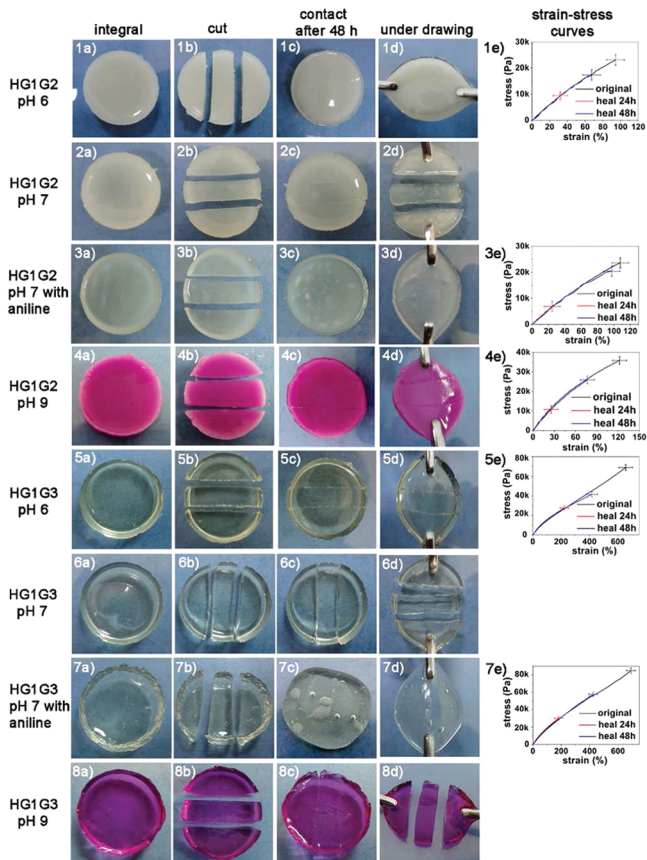


Figure 2. Self-healing properties of HG1G2 (10 wt %) and HG1G3 (10 wt %). Stress–strain curves of the five self-healable hydrogels (HG1G2 at pH 6, HG1G2 at pH 7 with aniline, HG1G2 at pH 9, HG1G3 at pH 6, and HG1G3 at pH 7 with aniline) are shown as 1e, 3e, 4e, 5e, and 7e.

turned red, indicating that it was basic (Figure 2-4a). The red HG1G2 pieces (Figure 2-4b) also self-healed into a whole plate in 48 h (Figure 2-4c) and could not be split (Figure 2-4d). The disulfide exchange reaction triggered by base is responsible for this self-healing process.^{20,26} It is worth noting that samples are self-healable only when a measurable dissociation rate constant is observed in the dynamic rheological tests (Figure 1a).

This adaptive self-healing mechanism of HG1G2 at different pH conditions was further confirmed by comparing the mechanism with the self-healing of HG1G3, which only contains acylhydrazone bonds. HG1G3 self-healed at the original state (pH 6) (Figure 2-5a–5d), further proving that the acylhydrazone exchange reaction is responsible for the self-healing under acidic conditions. At pH 7, HG1G3 could not repair itself (Figure 2-6a–6d), but when aniline was added, the HG1G3 pieces completely merged into a whole plate without visible cut lines in 48 h (Figure 2-7a–7d). As expected, HG1G3 could not repair itself in 20 days (Figure 2-8a–8d) under basic conditions (pH 9) by the same process used for HG1G2. This result proves that, without disulfide bonds in the gel, HG1G3 is not self-healable under basic conditions.

Tensile tests were performed to quantitatively evaluate the self-healing properties of the five self-healable hydrogels (Figure 2-1d, 3d, 4d, 5d, and 7d). Tensile tests were performed on the original and repaired samples after different healing times (24 or 48 h) (for sample preparation, test procedure, and video, see the SI). As shown in Figure 2 (1e, 3e, 4e, 5e, and 7e), stress–

strain curves of the original and self-healed hydrogels are almost superimposable for each pH condition, with the break stress and strain increasing with the healing time for all five cases. After 48 h of self-healing, the break stress and elongation values at break. The difference of the break elongation between HG1G2 and HG1G3 (Figure 2-1e–5e) is hypothesized to be generated by the structural differences between HG1G2 and HG1G3, that is, the additional disulfide bonds in HG1G2. Detailed reasons for this difference will be investigated in the future.

Aside from the tensile tests, self-healing cycles were practiced with the healed samples. After being cut again along the old cut lines, the resulting pieces of these samples self-healed in virtually the same manner as the first healing cycle.

In addition to self-healing properties, the HG1G2 hydrogel displayed interesting reversible sol–gel transitions in response to both pH and redox conditions. For pH responsive sol–gel transitions, HCl (5 M) and triethylamine were used as pH regulators. This transition process of HG1G2 (20 wt %) (Figure 3) was repeated four times (SI, Table S2). The pH

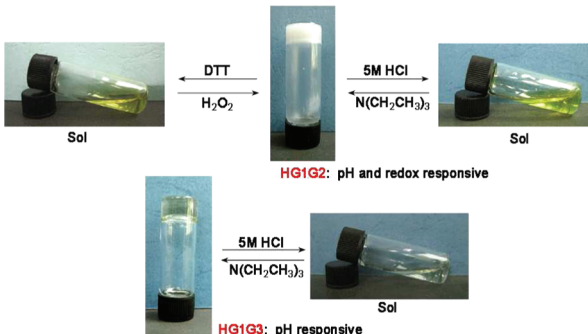


Figure 3. Sol–gel transitions of HG1G2 and HG1G3 in response to pH and/or redox triggers. The concentration of all of the samples was 20 wt %.

responsive sol–gel transition of HG1G3 was similar to that of HG1G2 (Figure 3 and Table S2), indicating that acylhydrazone bonds are responsible for the pH responsive sol–gel transition process. Redox responsive sol–gel transitions of HG1G2 were also reversible due to the disulfide bonds (Figure 3). Four transition cycles were repeated with DTT and H₂O₂ used as a reducer and oxidant, respectively (SI, Table S3). However, HG1G3 did not display responsive phase transitions to the redox stimuli. The pH and redox responsive sol–gel transitions were alternately connected. Four transition cycles were performed, two for pH and two for redox (SI, Table S4). The sequence of applying the stimuli (redox first or pH first) had no obvious effect on the transition cycle times.

In summary, we prepared polymer hydrogels containing both acylhydrazone and disulfide bonds and demonstrated that the orthogonal dynamic chemistry of the two bonds makes the hydrogel self-healable under a wide range of pH conditions (acidic, neutral, and basic). All of the self-healing processes were reversible and effective without an external stimulus at room temperature in air. The hydrogel was also reversible in sol–gel transitions in response to both pH and redox triggers. Following this idea of incorporating additional orthogonal dynamic bonds into the same system, more complex and unpredictable properties may be achieved in a single system. Such multiresponsive hydrogels will stimulate development of

smart soft materials that have potential applications in organ repair and stimuli-responsive drug delivery.

■ ASSOCIATED CONTENT

Supporting Information

Synthesis of the gelators, experimental methods, and relevant figures and tables. Two video files of tensile tests, HG1G3-pH6-original.avi and HG1G3-pH6-repaired-24 h.avi, are also provided. This material is available free of charge via the Internet at <http://pubs.acs.org>.

■ AUTHOR INFORMATION

Corresponding Author

*E-mail: ghdeng@scut.edu.cn; liucy@iccas.ac.cn; ymchen@iccas.ac.cn.

Notes

The authors declare no competing financial interest.

■ ACKNOWLEDGMENTS

This work is supported by the NSFC (No. 20974034, 21090353, 20874109) and the Guangdong Natural Science Foundation (No. 10351064101000000).

■ REFERENCES

- (1) Syrett, J. A.; Becer, C. R.; Haddleton, D. M. *Polym. Chem.* **2010**, *1*, 978–987.
- (2) Murphy, E. B.; Wudl, F. *Prog. Polym. Sci.* **2010**, *35*, 223–251.
- (3) White, S. R.; Sottos, N. R.; Geubelle, P. H.; Moore, J. S.; Kessler, M. R.; Sriram, S. R.; Brown, E. N.; Viswanathan, S. *Nature* **2001**, *409*, 794–797.
- (4) Toohey, K. S.; Sottos, N. R.; Lewis, J. A.; Moore, J. S.; White, S. R. *Nat. Mater.* **2007**, *6*, 581–585.
- (5) Rowan, S. J.; Cantrill, S. J.; Cousins, G. R. L.; Sanders, J. K. M.; Stoddart, J. F. *Angew. Chem., Int. Ed.* **2002**, *41*, 898–952.
- (6) Corbett, P. T.; Leclaire, J.; Vial, L.; West, K. R.; Wietor, J. L.; Sanders, J. K. M.; Otto, S. *Chem. Rev.* **2006**, *106*, 3652–3711.
- (7) Lehn, J. M. *Chem. Soc. Rev.* **2007**, *36*, 151–160.
- (8) Cordier, P.; Tournilhac, F.; Soulie-Ziakovic, C.; Leibler, L. *Nature* **2008**, *451*, 977–980.
- (9) Burattini, S.; Colquhoun, H. M.; Fox, J. D.; Friedmann, D.; Greenland, B. W.; Harris, P. J. F.; Hayes, W.; Mackay, M. E.; Rowan, S. *J. Chem. Commun.* **2009**, 6717–6719.
- (10) South, A. B.; Lyon, L. A. *Angew. Chem., Int. Ed.* **2010**, *49*, 767–771.
- (11) Maeda, T.; Otsuka, H.; Takahara, A. *Prog. Polym. Sci.* **2009**, *34*, 581–604.
- (12) Chen, X. X.; Dam, M. A.; Ono, K.; Mal, A.; Shen, H. B.; Nutt, S. R.; Sheran, K.; Wudl, F. *Science* **2002**, *295*, 1698–1702.
- (13) Nicolaï, R.; Kamada, J.; Van Wassen, A.; Matyjaszewski, K. *Macromolecules* **2010**, *43*, 4355–4361.
- (14) Amamoto, Y.; Kamada, J.; Otsuka, H.; Takahara, A.; Matyjaszewski, K. *Angew. Chem., Int. Ed.* **2011**, *50*, 1660–1663.
- (15) Deng, G.; Tang, C.; Li, F.; Jiang, H.; Chen, Y. *Macromolecules* **2010**, *43*, 1191–1194.
- (16) Bhat, V. T.; Caniard, A. M.; Luksch, T.; Brenk, R.; Campopiano, D. J.; Greaney, M. F. *Nat. Chem.* **2010**, *2*, 490–497.
- (17) Dirksen, A.; Dirksen, S.; Hackeng, T. M.; Dawson, P. E. *J. Am. Chem. Soc.* **2006**, *128*, 15602–15603.
- (18) Wojtecki, R. J.; Meador, M. A.; Rowan, S. J. *Nat. Mater.* **2011**, *10*, 14–27.
- (19) Otsuka, H.; Nagano, S.; Kobashi, Y.; Maeda, T.; Takahara, A. *Chem. Commun.* **2010**, *46*, 1150–1152.
- (20) Canadell, J.; Goossens, H.; Klumperman, B. *Macromolecules* **2011**, *44*, 2536–2541.
- (21) Orrillo, A. G.; Escalante, A. M.; Furlan, R. L. E. *Chem. Commun.* **2008**, 5298–5300.
- (22) Rodriguez-Docampo, Z.; Otto, S. *Chem. Commun. (Cambridge, U.K.)* **2008**, 5301–5303.
- (23) von Delius, M.; Geertsema, E. M.; Leigh, D. A. *Nat. Chem.* **2010**, *2*, 96–101.
- (24) Roberts, M.; Hanson, M.; Massey, A.; Karren, E.; Kiser, P. *Adv. Mater.* **2007**, *19*, 2503–2507.
- (25) Yount, W. C.; Loveless, D. M.; Craig, S. L. *J. Am. Chem. Soc.* **2005**, *127*, 14488–14496.
- (26) Danieli, B.; Giardini, A.; Lesma, G.; Passarella, D.; Peretto, B.; Sacchetti, A.; Silvani, A.; Pratesi, G.; Zunino, F. *J. Org. Chem.* **2006**, *71*, 2848–2853.